



Controlled Growth of Indium Selenides by High-Pressure and High-Temperature Method

Yajie Dai¹, Shouxin Zhao², Hui Han¹, Yafei Yan¹, Wenhui Liu¹, Hua Zhu¹, Liang Li¹, Xi Tang¹, Yang Li², Hui Li^{1*} and Changjin Zhang^{1,3}

¹Institute of Physical Science and Information Technology and Information Materials and Intelligent Sensing Laboratory of Anhui Province, Anhui University, Hefei, China, ²School of Materials Science and Engineering, Harbin Institute of Technology, Harbin, China, ³High Magnetic Field Laboratory of Anhui Province, Chinese Academy of Sciences, Hefei, China

The controlled growth of indium selenides has attracted considerable research interests in condensed matter physics and materials science yet remains a challenge due to the complexity of the indium–selenium phase diagram. Here, we demonstrate the successful growth of indium selenides in a controllable manner using the high-pressure and high-temperature growth technique. The γ -InSe and α -In₂Se₃ crystals with completely different stoichiometries and stacking manner of atomic layers have been controlled grown by subtle tuning growth temperature, duration time, and growth pressure. The as-grown γ -InSe crystal features a semiconducting property with a prominent photoluminescence peak of ~ 1.23 eV, while the α -In₂Se₃ crystal is ferroelectric. Our findings could lead to a surge of interest in the development of the controlled growth of high-quality van der Waal crystals using the high-pressure and high-temperature growth technique and will open perspectives for further investigation of fascinating properties and potential practical application of van der Waal crystals.

Keywords: indium selenides, controlled growth, high-pressure and high-temperature, photoluminescence, ferroelectricity

OPEN ACCESS

Edited by:

Zhaofu Zhang,
University of Cambridge,
United Kingdom

Reviewed by:

Hongchao Liu,
University of Macau, China
Kai Xu,
Zhejiang University, China

*Correspondence:

Hui Li
huili@ahu.edu.cn

Specialty section:

This article was submitted to
Computational Materials Science,
a section of the journal
Frontiers in Materials

Received: 17 November 2021

Accepted: 02 December 2021

Published: 11 January 2022

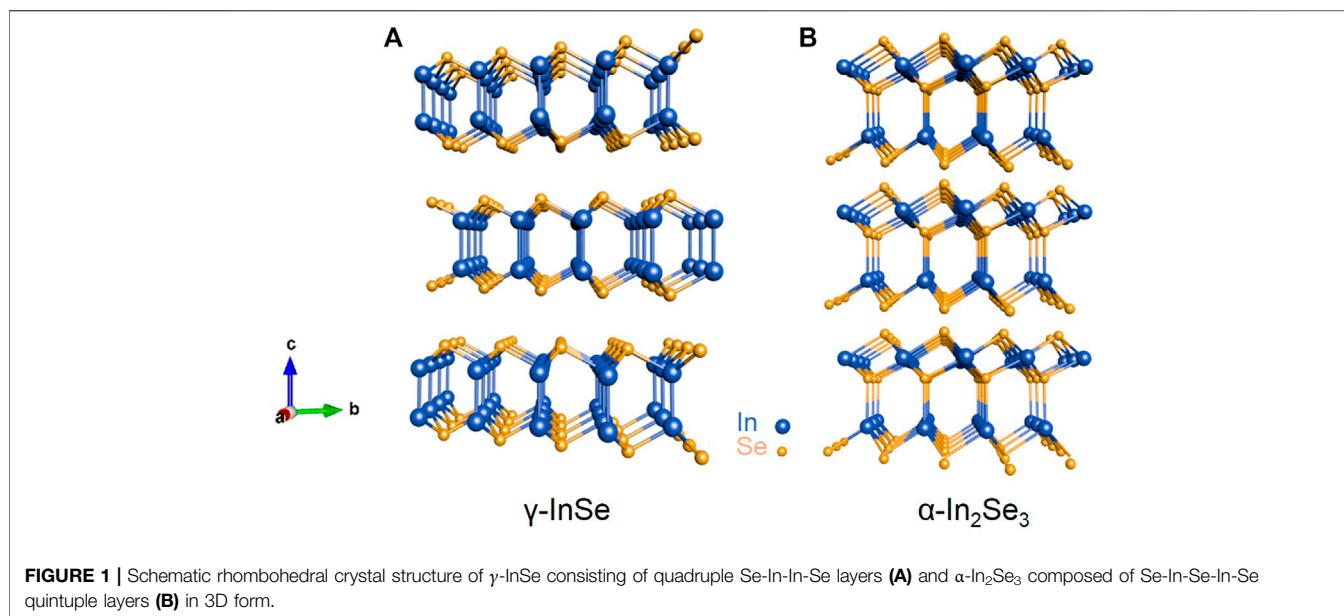
Citation:

Dai Y, Zhao S, Han H, Yan Y, Liu W,
Zhu H, Li L, Tang X, Li Y, Li H and
Zhang C (2022) Controlled Growth of
Indium Selenides by High-Pressure
and High-Temperature Method.
Front. Mater. 8:816821.
doi: 10.3389/fmats.2021.816821

INTRODUCTION

Indium selenides (In_xSe_y) are group III–VI semiconductors with kinds of In and Se stoichiometries and several structural modifications, for example, InSe with β , ϵ , and γ phases, and In₂Se₃ with α , β , γ , and σ phases (Butler et al., 2013; Bandurin et al., 2017; Balakrishnan et al., 2018). The rich tapestry of stoichiometries and structures of indium selenides makes them the treasure trove for fascinating properties with prospects in both frontier fundamental research and electronic device design, such as exotic ferroelectricity in α -In₂Se₃, ultrahigh electron mobility ($>10^4$ cm² V⁻¹ s⁻¹ at low temperature) of γ -InSe, and excellent photoresponsivity in β -InSe (Lei et al., 2014; Milutinović et al., 2016; Ding et al., 2017; Tang et al., 2019; Guo et al., 2020; Li et al., 2020; Ding et al., 2021).

Among them, γ -InSe and α -In₂Se₃ are two promising materials that have achieved considerable attention. Both γ -InSe and α -In₂Se₃ are layered structures with the intralayer being covalent bonded and the interlayers being interacted by van der Waals force, as shown in the schematic drawing of crystal structures in **Figure 1**. The γ -InSe consists of quadruple Se-In-In-Se layers in the rhombohedral stacking behavior (**Figure 1A**), while the α -In₂Se₃ is composed of Se-In-Se-In-Se quintuple layers arranged in a rhombohedral (R3m) crystal structure (**Figure 1B**) (Butler et al., 2013; Bandurin et al., 2017; Balakrishnan et al., 2018; Tang et al., 2019). Such different stacking behaviors of



In and Se atoms result in the γ -InSe and α -In₂Se₃ featuring distinct physical properties, which offers a new frontier of investigation on the relationship between the structures and properties. However, it is still a challenge to grow γ -InSe and α -In₂Se₃ in a controllable way because the energy difference between abundant structures of indium selenides is quite small.

Several approaches have been attempted to control grow γ -InSe and α -In₂Se₃, including chemical vapor deposition (CVD), chemical vapor transport (CVT), physical vapor deposition (PVD), pulse laser deposition (PLD), and the Bridgman method (Ishii, 1988; Zhou et al., 2016; Yang et al., 2017; Hu et al., 2018). Although substantial success has been achieved, the controlled growth of γ -InSe and α -In₂Se₃ still suffers from nonuniformity and time-consuming issues. Thus, the development of novel growth techniques is highly desirable. Recently, a few studies reported the utilization of the high-pressure and high-temperature (HPHT) growth method to grow the two-dimensional layered single crystals (Watanabe and Taniguchi, 2019). The high temperature and high pressure facilitate the crystallization and growth of crystals remarkably, which has provided an alternative and effective way toward the controlled growth of single crystals. However, the controlled growth of indium selenides using the HPHT technique has not been investigated. In this work, we systematically investigate the controlled growth of γ -InSe and α -In₂Se₃ using the HPHT growth technique by subtly adjusting the growth temperature, duration time, and the ratios of precursors. The photoluminescence (PL) of the as-grown γ -InSe and the ferroelectricity of the α -In₂Se₃ are further investigated.

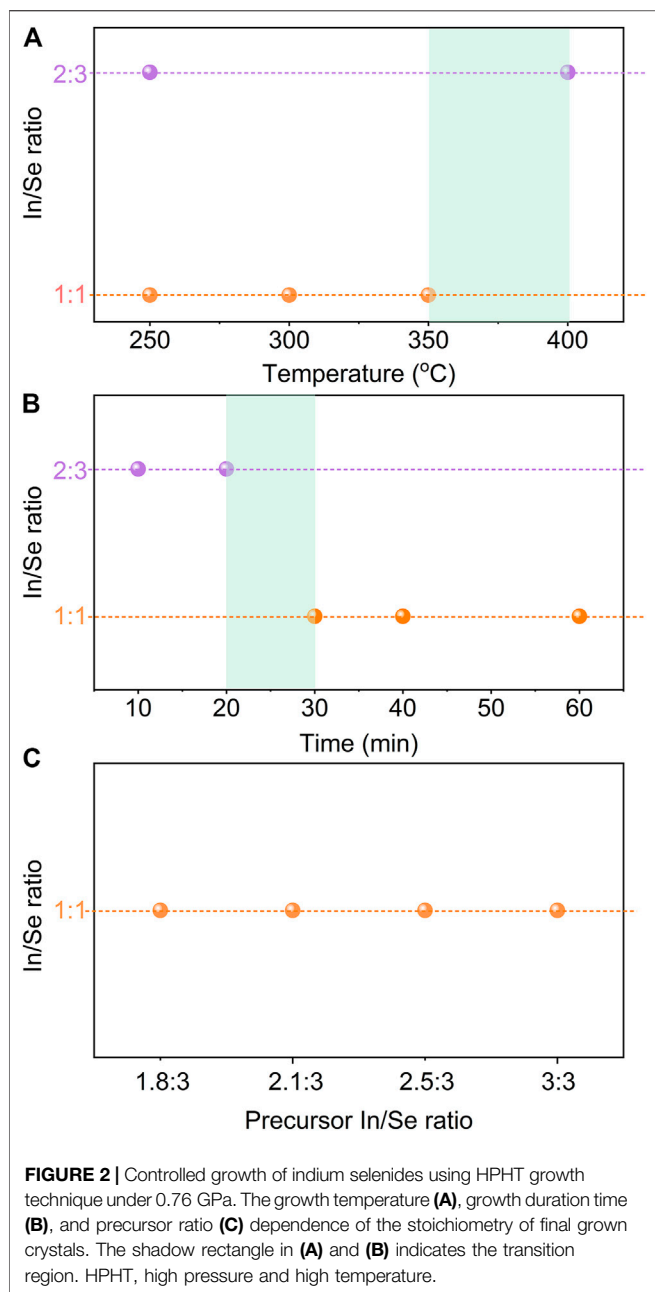
RESULTS AND DISCUSSION

The controlled growth of In_xSe_y crystals with different stoichiometries was realized by the HPHT growth technique.

Figure 2 summarizes the controlled growth of In_xSe_y crystals with different stoichiometries by subtle tuning growth temperature, duration time, and the ratios of precursors (precursor In/Se ratio) with the growth pressure of 0.76 GPa. As shown in **Figure 2A**, the crystalline In_xSe_y with mixed stoichiometries of 2:3 and 1:1 is obtained at 250°C with duration time of 20 min and precursor In/Se ratio of 2.1:3. Such a mixing behavior might be due to the nonuniform reaction under the relatively low growth temperature of 250°C, which is very close to the melting points of In (156.6°C) and Se (221°C). Importantly, if we increase the reaction temperature, the mixing behavior could be completely eliminated. As can be seen from **Figure 2A**, crystalline InSe with a stoichiometry of 1:1 could be obtained at growth temperature of 300°C and 350°C, while the crystalline In₂Se₃ with a stoichiometry of 2:3 is eventually achieved as the growth temperature further increases to 400°C with other growth conditions unchanged. The present results are in principle consistent with the provisional equilibrium In-Se binary phase diagram (Lu et al., 1999), in which In₂Se₃ crystals are preferred to be formed at relatively high temperatures.

We further demonstrate that the stoichiometry of the obtained crystals could be effectively modulated by the growth duration time. As shown in **Figure 2B**, the stoichiometry of the obtained crystals changes from 2:3 (i.e., In₂Se₃) to 1:1 (i.e., InSe) with the growth duration time increasing from 10 to 30 min under 0.76 GPa and 400°C with precursor In/Se ratio of 2.1:3, indicating that the longer growth duration time is beneficial for the growth of InSe crystals. Further increasing duration time to 60 min does not change the stoichiometry of the obtained crystals.

In contrast to the growth temperature and duration time, the In/Se ratios of the precursors have no influence on the stoichiometry of the resultant crystals. The InSe crystals with a stoichiometry of 1:1 are obtained even with the precursor In/Se ratio changes in a wide range from 1.8:3 to 3:3 under the growth condition of 0.76 GPa, 400°C, and duration time of 30 min (**Figure 2C**).



We perform a systematical investigation on the growth of In_xSe_y crystal with a controlled stoichiometry by adjusting the growth conditions, including growth pressure, duration time, and precursor ratios. As summarized in **Supplementary Table S1**, no bulk crystalline products were obtained under growth pressure above 2 GPa with various kinds of growth temperatures, growth duration time, and precursor In/Se ratio. This fact suggests that the high pressure above 2 GPa is not favorable in the growth of In_xSe_y crystals.

Figure 3 shows the optical images and scanning electron microscopy (SEM) images of the obtained crystals grown under 0.76 GPa and 400°C with In/Se precursor ratio of 2.1:3 for 30 and 10 min. The stoichiometry of the crystals is determined to be

InSe (**Figure 3A**) and In_2Se_3 (**Figure 3B**) by the energy-dispersive X-ray spectroscopy (EDS) analysis, as shown in **Supplementary Figure S1**. The as-grown crystals are shiny with large sizes of about 5×1.6 mm for InSe (**Figure 3A**) and of about 1.7×1.3 mm for In_2Se_3 (**Figure 3B**). In addition, the resultant crystals exhibit clearly layered structures, as shown in the SEM images in **Figures 3C,D**.

Raman spectra were utilized to identify the phases of the InSe and In_2Se_3 crystals, as indicated in **Figure 4**. Four Raman modes, namely, A_{1g}^1 at 114 cm^{-1} , E_{2g}^1 at 177 cm^{-1} , $A_{1g}^1(\text{LO})$ at 198 cm^{-1} , and A_{1g}^2 at 226 cm^{-1} , are clearly seen for InSe flakes, which suggests the as-grown InSe crystals are of γ -phase (**Figure 4A**) (Balakrishnan et al., 2018; Wu et al., 2019; Mudd et al., 2013). For In_2Se_3 , three Raman peaks located at 103, 180, and 193 cm^{-1} are observed (**Figure 4B**), which can be ascribed to $A_1(\text{LO} + \text{TO})$, $A_1(\text{TO})$, and $A_1(\text{TO})$ phonon modes, respectively, of rhombohedral α - In_2Se_3 with space group of $R3m$, as indicated in **Figure 1B** (Lewandowska et al., 2001). Generally, E modes correspond to the in-plane vibration modes, while A modes correspond to the out-of-plane vibration modes. In α - In_2Se_3 , only A modes are observed, which is probably due to the parallel measurement configuration of Raman measurement so that the wave vector of the exciting light is parallel to the c -axis of the α - In_2Se_3 (Lewandowska et al., 2001).

The crystal structures of the single crystals are further investigated by transmission electron microscopy (TEM). The thin γ -InSe and α - In_2Se_3 flakes were transferred on Cu grids by mechanical exfoliation and standard wet transfer method. **Figure 5A** shows the morphology of γ -InSe flakes. The selected area electron diffraction pattern (**Figure 5B**) measured in the marked area (red ellipse in **Figure 5A**) shows a six-fold symmetry, which suggests that the InSe crystals are of hexagonal structure. The high-resolution TEM image of the InSe flake clearly shows the hexagonal structure with the angle between the well-recognized a and b axes at 120° (**Figure 5C**). The lattice constant is determined to be about 0.4 nm, which is consistent with the lattice spacing of layered γ -InSe ($a = b = 4.005 \text{ \AA}$, $c = 24.96 \text{ \AA}$) (Chen et al., 2015). The same TEM investigations were also carried out on α - In_2Se_3 flakes, as shown in **Figures 5D-F**. The lattice constant is measured to be about 0.35 nm, which corresponds to d -spacing (100) lattice planes of α - In_2Se_3 (Ho et al., 2013; Zhou et al., 2015; Feng et al., 2016; Zhou et al., 2017; Tang et al., 2019).

Figure 6 shows the PL spectra of the γ -InSe flakes exfoliated from the as-grown crystals. A prominent peak at $\sim 1.23 \text{ eV}$ is observed for ~ 22 -nm γ -InSe (**Figure 6A**). The thickness of γ -InSe flake is determined by the atomic force measurement, as shown in **Supplementary Figure S2**. By increasing the excitation laser power, the PL peak intensity increases. The excitation power dependence of the PL peak intensity follows the power law, $I \propto P^k$, in which I , P , and k are integrated peak intensity, excitation laser power, and power-law index, respectively. As shown in the log-log plot in **Figure 6B**, the value of k is fitted to be about 0.5. This suggests that the recombination is most likely originated from the localized electron-hole pairs in the γ -InSe, which is consistent with

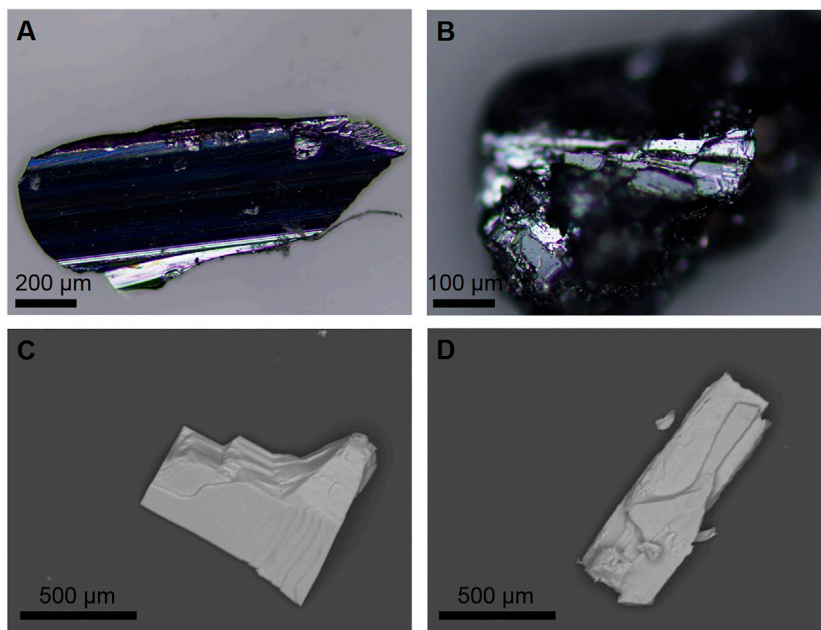


FIGURE 3 | Optical images of as-grown InSe crystal (A) and In₂Se₃ crystal (B). SEM image of InSe crystal (C) and In₂Se₃ crystal (D) exfoliated on SiO₂ substrate. SEM, scanning electron microscopy.

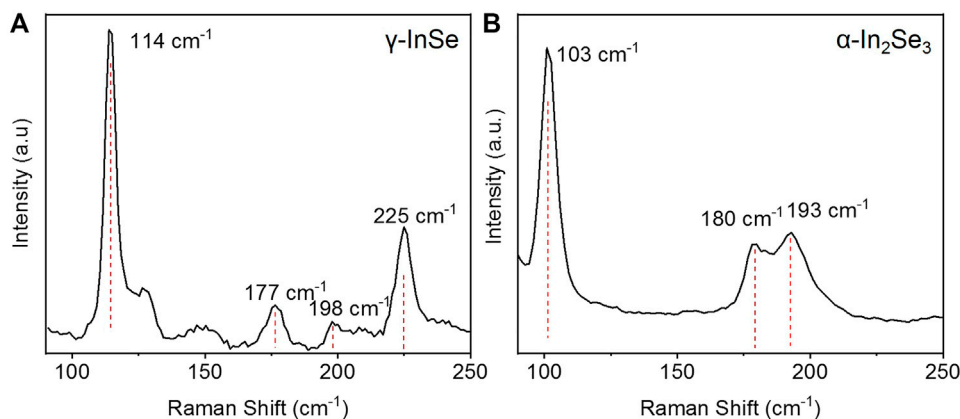


FIGURE 4 | Micro-Raman spectra of γ -InSe flake (A) and α -In₂Se₃ flake (B) with excitation laser wavelength of 532 nm.

the theoretical calculations for the phonon sideband emission process (Brener et al., 1992). A similar semiconducting property with a prominent PL peak at ~ 1.37 eV is also observed for α -In₂Se₃ flake, as shown in **Supplementary Figure S3**.

The piezoelectricity of the as-grown α -In₂Se₃ has been further investigated by the piezoresponse force microscopy (PFM) measurements. **Figure 7** shows the out-of-plane PFM amplitude (**Figure 7A**) and phase image (**Figure 7B**). The high and low amplitudes are clearly observed in the inner square and outer square, respectively, which corresponds to the opposite polarization states after writing with +7 V and -5 V, respectively. In addition, the domain wall between the oppositely polarized region is clear

and does not coincide with the edges of the samples, which excludes the contribution of other artifact effects.

CONCLUSION

The controlled growth of indium selenide crystals was achieved successfully using the HPHT growth technique. The stoichiometry and structure of the indium selenides were well controlled by tuning the growth temperature and duration time at specific growth pressure of 0.76 GPa. The relatively low growth temperature and long duration time are beneficial for the growth of γ -InSe. On the contrary, α -In₂Se₃ crystals could be

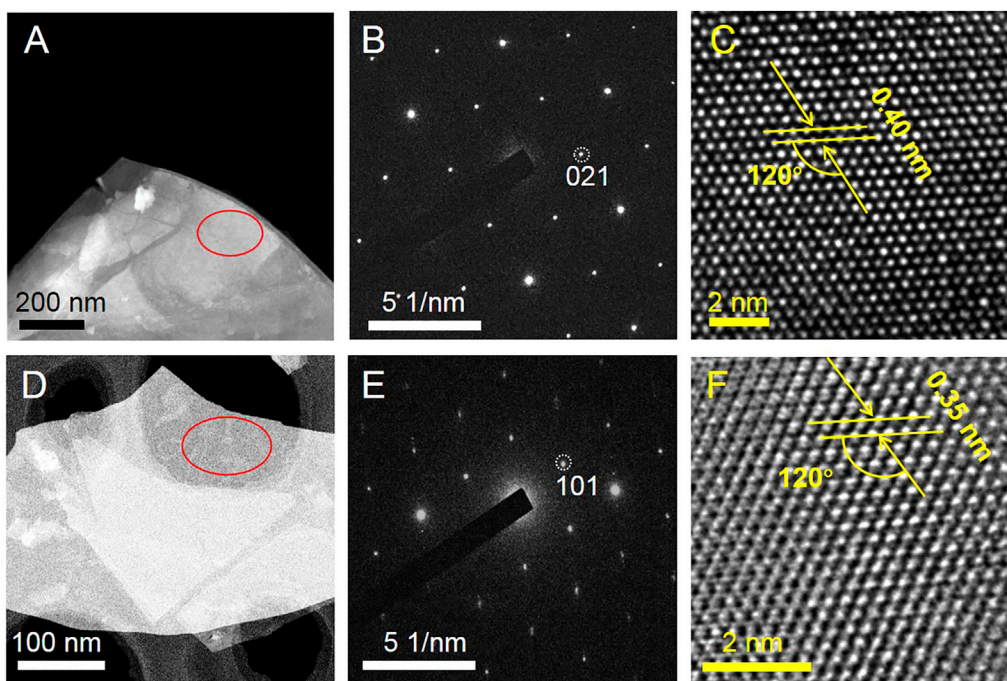


FIGURE 5 | (A) TEM image of γ -In₂Se₃ flake. **(B)** SAED pattern and **(C)** HR-TEM image of γ -In₂Se₃ flake collected in the marked area in **(A)**. **(D)** TEM image of α -In₂Se₃ flake. **(E)** SAED pattern and **(F)** HR-TEM image of α -In₂Se₃ flake collected in the marked area in **(D)**. TEM, transmission electron microscopy; SAED, selected area electron diffraction; HR-TEM, high-resolution TEM.

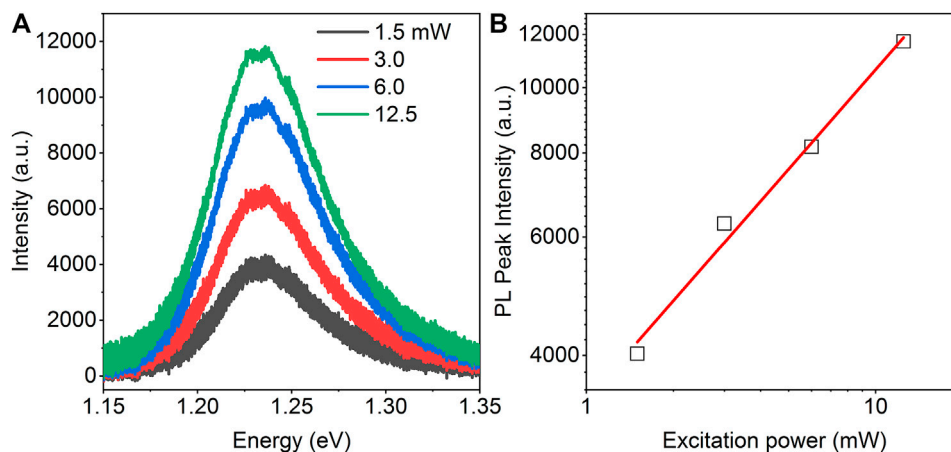


FIGURE 6 | (A) Photoluminescence (PL) spectra of the γ -In₂Se₃ flake of about 22 nm at different incident laser power indicated. **(B)** Log-log plot of PL intensity as a function of the excitation power. The solid red line is the linear fitting curve with power-law index of ~ 0.5 .

easily obtained at relatively high growth temperature and short growth duration time. Moreover, diverse physical properties were observed in the resultant crystals; i.e., γ -In₂Se₃ shows a prominent PL peak at ~ 1.23 eV, and α -In₂Se₃ exhibits evident ferroelectricity, which holds promise for the potential applications in optoelectronics and ferroelectric memory devices. Our findings have provided an alternative strategy for crystals growth in a controlled manner and will stimulate further development of high-quality crystal growth with

numerous fascinating physical properties and functional device applications.

METHODS

Characterization

Structural investigations and stoichiometry analyses of as-grown crystals were determined by EDS analysis through a field-emission

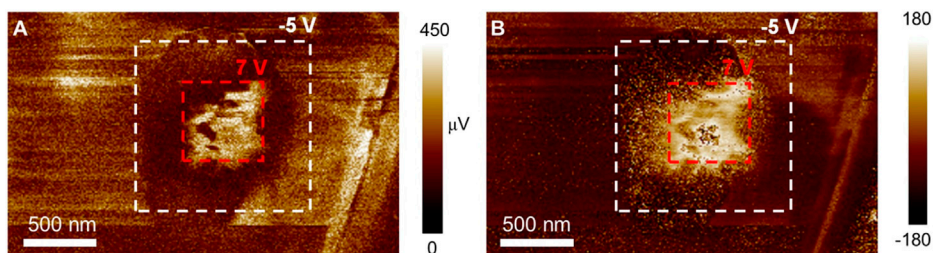


FIGURE 7 | The out-of-plane PFM amplitude (A) and phase (B) of as-grown α -In₂Se₃ flake exfoliated on SiO₂ substrate. The red and white dashed areas are polarized using different driving voltages of +7 V and -5 V, respectively. PFM, piezoresponse force microscopy.

SEM (JEOL-7100F, JEOL Ltd, Tokyo, Japan) at room temperature. The high-resolution images are measured by TEMs (JEM 2100; JEOL) with an acceleration voltage of 200 kV. The PL spectra were collected on micro-Raman/PL system (InVia, Renishaw, Wotton-under-Edge, UK) using an argon green laser at 514 nm. PFM measurements were performed in ambient conditions by using scanning probe microscopies (Bruker Dimension Icon-PT, Kontich, Belgium). Co/Cr tips (MESP, Bruker) were used for PFM measurements. An ac driving voltage of 0.5–1 V at a near resonance frequency of 280–400 kHz was applied to collect the PFM domain images (PFM phase and amplitude).

DATA AVAILABILITY STATEMENT

The raw data supporting the conclusion of this article will be made available by the authors, without undue reservation.

AUTHOR CONTRIBUTIONS

HL conceived the project. YD grew and characterized the crystals with support from HH, YL, WL, HZ, XT, SZ and

YL. All authors contributed to the article and approved the submitted version.

FUNDING

This work was supported in part by the National Natural Science Foundation of China under Grant Nos. 11904001 and 51902069, the Joint Funds of the National Natural Science Foundation of China and the Chinese Academy of Sciences Large-Scale Scientific Facility under Grant No. U1932156, the Natural Science Foundation of Anhui Province under Grant No. 2008085QA29, and the Project of Science and Technology on Reliability Physics and Application Technology of Electronic Component Laboratory under Grant No. 61428060101.

SUPPLEMENTARY MATERIAL

The Supplementary Material for this article can be found online at: <https://www.frontiersin.org/articles/10.3389/fmats.2021.816821/full#supplementary-material>

REFERENCES

- Balakrishnan, N., Steer, E. D., Smith, E. F., Kudrynskiy, Z. R., Kovalyuk, Z. D., Eaves, L., et al. (2018). Epitaxial Growth of γ -InSe and α , β , and γ -In₂Se₃ on ϵ -GaSe. *2d Mater.* 5, 035026. doi:10.1088/2053-1583/aac479
- Bandurin, D. A., Tyurnina, A. V., Yu, G. L., Mishchenko, A., Zólyomi, V., Morozov, S. V., et al. (2017). High Electron Mobility, Quantum Hall Effect and Anomalous Optical Response in Atomically Thin InSe. *Nat. Nanotech* 12, 223–227. doi:10.1038/nnano.2016.242
- Brener, I., Olszakier, M., Cohen, E., Ehrenfreund, E., Ron, A., and Pfeiffer, L. (1992). Particle Localization and Phonon Sidebands in GaAs/AlxGa1-xAs Multiple Quantum wells. *Phys. Rev. B* 46, 7927–7930. doi:10.1103/physrevb.46.7927
- Butler, S. Z., Hollen, S. M., Cao, L., Cui, Y., Gupta, J. A., Gutiérrez, H. R., et al. (2013). Progress, Challenges, and Opportunities in Two-Dimensional Materials beyond Graphene. *ACS Nano* 7, 2898–2926. doi:10.1021/nn400280c
- Chen, Z., Biscaras, J., and Shukla, A. (2015). A High Performance Graphene/few-Layer InSe Photo-Detector. *Nanoscale* 7, 5981–5986. doi:10.1039/c5nr004000d
- Ding, J., Shao, D. F., Li, M., Wen, L. W., and Tsymbal, E. Y. (2021). Two-dimensional Antiferroelectric Tunnel junction. *Phys. Rev. Lett.* 126, 057601. doi:10.1103/PhysRevLett.126.057601
- Ding, W., Zhu, J., Wang, Z., Gao, Y., Xiao, D., Gu, Y., et al. (2017). Prediction of intrinsic two-dimensional ferroelectrics in In₂Se₃ and other III₂-VI₃ van der Waals materials. *Nat. Commun.* 8, 14956. doi:10.1038/ncomms14956
- Feng, W., Zheng, W., Gao, F., Chen, X., Liu, G., Hasan, T., et al. (2016). Sensitive Electronic-Skin Strain Sensor Array Based on the Patterned Two-Dimensional α -In₂Se₃. *Chem. Mater.* 28, 4278–4283. doi:10.1021/acs.chemmater.6b01073
- Guo, H., Zhang, Z., Huang, B., Wang, X., Niu, H., Guo, Y., et al. (2020). Theoretical study on the photocatalytic properties of 2D InX(X = S, Se)/transition metal disulfide (MoS₂ and WS₂) van der Waals heterostructures. *Nanoscale* 12, 20025–20032. doi:10.1039/d0nr04725b
- Ho, C.-H., Lin, C.-H., Wang, Y.-P., Chen, Y.-C., Chen, S.-H., and Huang, Y.-S. (2013). Surface Oxide Effect on Optical Sensing and Photoelectric Conversion of α -In₂Se₃ Hexagonal Microplates. *ACS Appl. Mater. Inter.* 5, 2269–2277. doi:10.1021/am400128e
- Hu, Y., Feng, W., Dai, M., Yang, H., Chen, X., Liu, G., et al. (2018). Temperature-dependent Growth of Few Layer β -InSe and α -In₂Se₃ Single Crystals for Optoelectronic Device. *Semicond. Sci. Technol.* 33, 125002. doi:10.1088/1361-6641/aae629
- Ishii, T. (1988). High Quality Single crystal Growth of Layered InSe Semiconductor by bridgman Technique. *J. Cryst. Growth* 89, 459–462. doi:10.1016/0022-0248(88)90206-0

- Lei, S., Ge, L., Najmaei, S., George, A., Koppera, R., Lou, J., et al. (2014). Evolution of the Electronic Band Structure and Efficient Photo-Detection in Atomic Layers of InSe. *ACS Nano*. 8, 1263–1272. doi:10.1021/nn405036u
- Lewandowska, R., Bacewicz, R., Filipowicz, J., and Paszkowicz, W. (2001). Raman Scattering in α -In₂Se₃ Crystals. *Mater. Res. Bull.* 36, 2577–2583. doi:10.1016/s0025-5408(01)00746-2
- Li, Y.-H., Yu, C.-B., Li, Z., Jiang, P., Zhou, X.-Y., Gao, C.-F., et al. (2020). Layer-dependent and Light-Tunable Surface Potential of Two-Dimensional Indium Selenide (InSe) Flakes. *Rare Met.* 39, 1356–1363. doi:10.1007/s12598-020-01511-4
- Lu, K., Sui, M. L., Perepezko, J. H., and Lanning, B. (1999). The Kinetics of Indium/amorphous-Selenium Multilayer Thin Film Reactions. *J. Mater. Res.* 14, 771–779. doi:10.1557/jmr.1999.0103
- Milutinović, A., Lazarević, Z. Z., Jakovljević, M., Hadžić, B., Petrović, M., Petrović, M., et al. (2016). Optical Properties of Layered III-VI Semiconductor γ -InSe: M (M=Mn, Fe, Co, Ni). *J. Phys. Chem. Sol.* 86, 120–127.
- Mudd, G. W., Svatek, S. A., Ren, T., Patané, A., Makarovskiy, O., Eaves, L., et al. (2013). Tuning the Bandgap of Exfoliated InSe Nanosheets by Quantum Confinement. *Adv. Mater.* 25, 5714–5718. doi:10.1002/adma.201302616
- Tang, L., Teng, C., Luo, Y., Khan, U., Pan, H., Cai, Z., et al. (2019). Confined van der Waals Epitaxial Growth of Two-Dimensional Large Single-Crystal In₂Se₃ for Flexible Broadband Photodetectors. *Research* 2019, 1–10. doi:10.1155/2019/2763704
- Watanabe, K., and Taniguchi, T. (2019). Far-UV Photoluminescence Microscope for Impurity Domain in hexagonal-boron-nitride Single Crystals by High-Pressure, High-Temperature Synthesis. *Npj 2d Mater. Appl.* 3, 40. doi:10.1038/s41699-019-0124-4
- Wu, M., Xie, Q., Wu, Y., Zheng, J., Wang, W., He, L., et al. (2019). Crystal Structure and Optical Performance in Bulk γ -InSe Single Crystals. *AIP Adv.* 9, 025013. doi:10.1063/1.5086492
- Yang, Z., Jie, W., Mak, C.-H., Lin, S., Lin, H., Yang, X., et al. (2017). Wafer-scale Synthesis of High-Quality Semiconducting Two-Dimensional Layered InSe with Broadband Photoresponse. *ACS Nano*. 11, 4225–4236. doi:10.1021/acsnano.7b01168
- Zhou, J., Zeng, Q., Lv, D., Sun, L., Niu, L., Fu, W., et al. (2015). Controlled Synthesis of High-Quality Monolayered α -In₂Se₃ via Physical Vapor Deposition. *Nano. Lett.* 15, 6400–6405. doi:10.1021/acs.nanolett.5b01590
- Zhou, S., Tao, X., and Gu, Y. (2016). Thickness-Dependent Thermal Conductivity of Suspended Two-Dimensional Single-Crystal In₂Se₃ Layers Grown by Chemical Vapor Deposition. *J. Phys. Chem. C* 120, 4753–4758. doi:10.1021/acs.jpcc.5b10905
- Zhou, Y., Wu, D., Zhu, Y., Cho, Y., He, Q., Yang, X., et al. (2017). Out-of-Plane Piezoelectricity and Ferroelectricity in Layered α -In₂Se₃ Nanoflakes. *Nano. Lett.* 17, 5508–5513. doi:10.1021/acs.nanolett.7b02198

Conflict of Interest: The authors declare that the research was conducted in the absence of any commercial or financial relationships that could be construed as a potential conflict of interest.

Publisher's Note: All claims expressed in this article are solely those of the authors and do not necessarily represent those of their affiliated organizations, or those of the publisher, the editors, and the reviewers. Any product that may be evaluated in this article, or claim that may be made by its manufacturer, is not guaranteed or endorsed by the publisher.

Copyright © 2022 Dai, Zhao, Han, Yan, Liu, Zhu, Li, Tang, Li, Li and Zhang. This is an open-access article distributed under the terms of the Creative Commons Attribution License (CC BY). The use, distribution or reproduction in other forums is permitted, provided the original author(s) and the copyright owner(s) are credited and that the original publication in this journal is cited, in accordance with accepted academic practice. No use, distribution or reproduction is permitted which does not comply with these terms.